Ocean Engineering 195 (2020) 106699

Contents lists available at ScienceDirect

Ocean Engineering

journal homepage: www.elsevier.com/locate/oceaneng

Performance evaluation of a drag hydro kinetic turbine for rivers current energy extraction - A case study

A. Ramadan [a,*], Mohamed A.A. Nawar [b], M.H. Mohamed [b,c]

[a] College of Engineering and Technology, Arab Academy for Science and Technology and Maritime Transport (AAST), Cairo, Egypt
[b] Faculty of Engineering-Mattaria, Helwan University, Cairo, Egypt
[c] Mechanical Engineering Dept, College of Engineering and Islamic Architecture, Umm Al-Qura University, P.O. 5555, Makkah, Saudi Arabia

ARTICLE INFO

Keywords:
River current
River nile
Vertical axis turbine
Hydro-kinetic energy

ABSTRACT

River current energy is considered as the greenest energy available, as it has enormous energies stored. It is a promising energy source in renewable energy due to the accessibility and availability. The River Nile in Egypt has been selected in this work as the case study for this kind of energy. The process of hydro-kinetic energy conversion utilizes the contained kinetic energy in the river stream which can be extracted by a submerged vertical axis turbine. The main objective of this work is to design and simulate a water current stream energy conversion system as a stand-alone power station for the electric power generation. The generated electric power is intended for rural and domestic applications. CFD is used to simulate and redesign a drag turbine. The numerical analysis indicates that the S shape blade has the maximum power coefficient of 24.6% for a tip speed ratio 0.8 and streamflow velocity 3 m/s. The results indicate that the maximum power coefficient of the S shape and the conventional design are 18% and 12.8% respectively at the tip speed ratio 0.8 and 0.5 m/s. The S shape enhances the turbine performance by 40% compared with the conventional design, especially at low velocity.

1. Introduction

The captured energy from the river stream is being considered as a pivotal source of renewable energy. The vertical axis turbine system is considered as a new and an emerging category of renewable energy technology and in remote areas, an unconventional solution for electric power production (Antheaume et al., 2008). The water current stream energy (WCSE) conversion system will be considered as the first station conducted in Egypt and in the Middle East at all. The construction of these stations and the prosperity of this type of electric power stations will contribute to the development of Upper Egypt in many fields like Agriculture, tourism, and industry. The main problem is that the Ministry of Electricity & Renewable Energy at Egypt does not have the vision or the strategy for the wave and water current stream energy conversion to generate electric power. However, this article encourages and introduces this type of renewable energy to draw attention to use it. Water turbines shapes were born from wind turbines with both types of vertical and horizontal axis turbines (Antheaume et al., 2008).

The high performance with high power production is introduced by a smooth linear flow of water at high velocity (laskan Inc. report, 2010). The flow features and characteristics of any river stream have some variation, seasonal and daily, and the installation of the water current turbine should be indeed considered. The main feature of the river flow is unidirectional flow and this eliminates the need for yaw adjustments. The hydrokinetic converter and the level of power output are directly affected by the water velocity. The location and the position of the hydrokinetic device have a relation to the cross-section of the flow channel. Moreover, it is a very important and significant component for two essential reasons. First, depending on the river's bottom depth, the energy flux at the surface of the water is stronger than the river's bottom. In addition, this quantity takes diverse values depending on the distance from the shore. In a smooth channel, the water current is fastest at the center, but in a river, this may vary depending on river bathymetry. Therefore, the water velocity has a certain site-specific and localized profile, where the available amount of energy flux that can be obtained that can be produced depends on the rotor location (Antheaume et al., 2008). Second, many river users are competing inside the water flow, such as boats, fishing vessels, bridges, etc., and these might reduce the efficiency and effectiveness of the useable area for a turbine installation (laskan Inc. report, 2010). In addition, other types of suspended and hanged particles and materials such as rock, fish, etc. in the river (Verdant Power, 2006) could also be varying.

* Corresponding author.
E-mail address: ahmedramadan2001@aast.edu (A. Ramadan).

https://doi.org/10.1016/j.oceaneng.2019.106699
Received 1 June 2019; Received in revised form 11 October 2019; Accepted 7 November 2019
Available online 15 November 2019

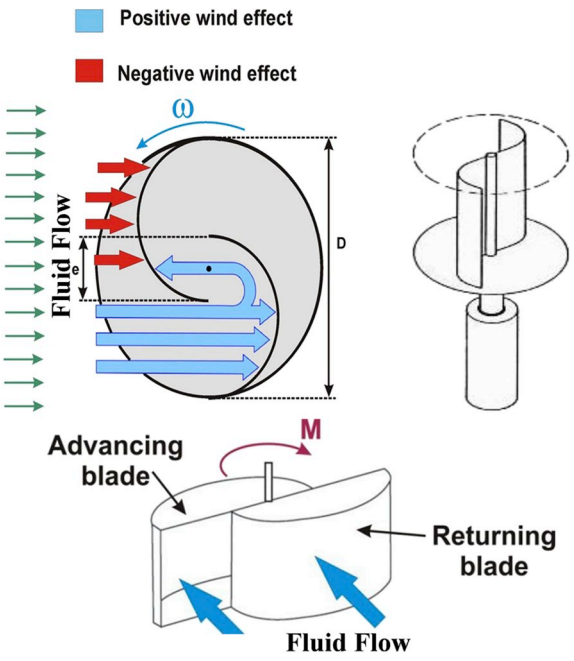

Fig. 1. Savonius turbine's Blade and flow direction (Mohamed, 2011).

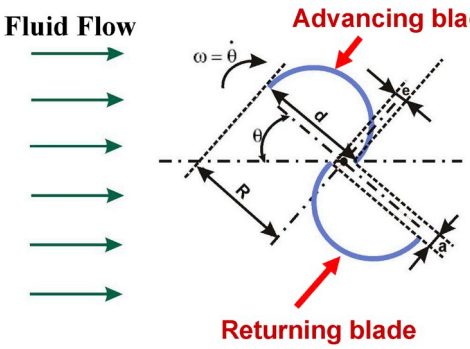

Fig. 2. The deflector design impeded with the Savonius hydrokinetic turbine (Mohamed, 2011).

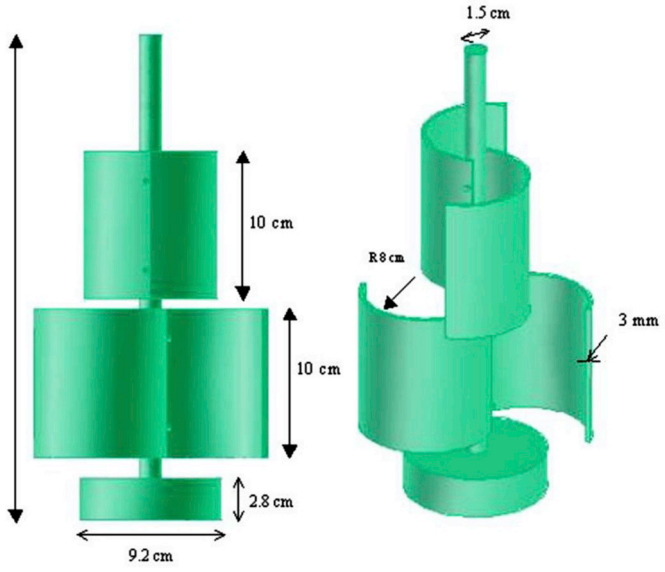

Fig. 3. The physical model of the 2-stage 2-bladed Savonius rotor.

A vertical axis turbine (Fig. 1) is considered for deployment at this location in lieu of a horizontal axis turbine for the following reasons:

1. Energy flux has a high due at the near of the surface of the river.
2. The effect and influence of competing users from fishing and boating are avoided.
3. Footprint: any trenching, pilling at the bottom may become subject to the environmental scrutiny.
4. The foundation and structure of vertical axis turbine are very low compared to the horizontal axis turbine.
5. Low cost and high durability.
6. The manufacturing of this type especially the S-shaped is available locally at Egypt (Blue Power Co.).
7. The power production is continuous around the year with just a small adaptation to the water level.

Tutar and Veci (2015) investigated the effect of water depths with different wave boundary conditions on the performance of Savonius turbine with single and multiple turbine arrays, (3 turbines) with three various positions of arrays. However, these arrays were conducted at several distances between them. The submersion depth of the turbine blade underwater line had an influence on the rotor performance. The rotor was fabricated with three blades, each of which is made of a 2 mm aluminum sheet and is bent at a blade angle of 59°. The blades were mounted on a 16.0 mm diameter shaft. The rotor had a width of w = 480 mm and an outer diameter of d = 252 mm.

The submersion level was −5, 0 and 5 cm with a rotor diameter of 25 cm. They built the experimental model and tested it under a certain condition of water waves. They concluded that the three blades rotor with 0 level (center of rotor on water surface) submersions had a maximum efficiency of 18% compared to 8% at −5 cm.

On the other side, Sarma and et al. (Sarma et al., 2014) conducted a numerical model of the Savonius hydrokinetic turbine (Drag type). Moreover, they tested it experimentally. The experimental work was performed at the water channel with a water speed range from 0.3 to 0.9 m/s. They compared the produced power output from the same turbine in water and wind, showing how the generated output power from water was greater than wind. The power ratio between water and wind was calculated to be 61.32% with the turbine. Otherwise, the simulation was done using the CFD program with maximum power coeffiecnt of 9%. Yaakob and et al. (Yaakob et al., 2013) studied the effect of the deflectors on the Savonius hydrokinetic turbine inside a duct. They had two different designs of deflectors; the first one had one deflector, and the second had two deflectors as in Fig. 2. The three-dimensional CFD analysis was chosen by the authors, to study and investigate the power and torque coefficient. The power coefficient is defined as the ratio between the output power from the turbine by torque and angular velocity on the rotor to the incident power from the water stream on the blade according to the velocity of water stream. The power coefficient was 0.27 in two deflectors compared to which equals 0.21 for only one deflector, this increase in the C_p indicated the influence of these deflectors on the whole performance of the Savonius hydrokinetic turbine.

Sharma and et al. (Sharma et al., 2014) reported the enhancement of the conventional Savonius hydrokinetic turbine's efficiency of 21% as a maximum by controlling its design parameters. The performance and characteristics of a two-stage, two-bladed configuration of the Savonius rotor had been investigated. Whole experiments had been carried out in a wind tunnel which has low wind speed. The studied parameters were the overlap ratio, tip speed ratio, power coefficient (C_p) and torque coefficient (C_t) as shown and illustrated in Fig. 3. The study showed that a maximum C_p of 0.517 was obtained at 9.37% overlap condition. The overlap condition is meant that, the both turbines had different installation angle to each other and to the incident air on them.

Schleicher and et al. (Chris Schleicher et al., 2013) worked numerically as a 3D simulation to generate 500 Watt from the water current.

Fig. 4. The selected locations for a water turbine.

The turbine had the captured efficiency of 0.45 at a rotor diameter of 0.5334 m with water speed less than 2.2 m/s.

Zaidi and et al. (Zaidi et al., 2013) investigated the effect of the chord length of the helical blade 3D numerical simulation on the performance of the turbine (Grolov Turbine). This study was conducted and carried out by utilizing the commercial code fluent of ANSYS; this investigation was performed by employing the shear stress transport (SST) k-ω model. They used the hydrofoil of NACA 0012 with rotor radius 0.15 m with chord lengths of 0.006, 0.0983, and 0.0988 m. The data output from the 3D numerical simulation showed that the maximum C_p was 58% at chord length 0.0983 m. Hantoro and et al. (Hantoro et al., 2018) performed an experimental study at an open channel to investigate an innovative design for the Darrius type to be a hydrokinetic turbine. They compared the convention one with 3 straight blades and two designs with 6 and 9 blades (SBC), where the swept area was the same for all. The power coefficient for the 9 blades design was 0.42 at TSR 2.91 which is the maximum could be reached for the system.

Kumar and Sini (Kumar and Saini, 2017) carried out enhancement on the performance of the Savonius hydrokinetic turbine using CFD analysis. The simulation and calculations of the twisted Savonius hydrokinetic turbine had been introduced and carried out by the commercial unsteady Reynolds-Averaged Navier-Stokes (URANS) solver in conjunction with a realizable k-ε turbulence model. It had been found that Savonius hydrokinetic turbine having a twist angle of 12.5°, which produces an optimum power coefficient, equals 0.39 at speed ratio equals to 0.9 with a water velocity of 2 m/s. It was found that, Savonius hydrokinetic turbine with a twist angle of 12.5° produces an optimum power coefficient of 0.39 at a tip speed ratio and water velocity of 0.9 and 2 m/s, respectively.

As appeared in all the previous work, design, and shapes of the blades are a very important factor for most of the energy conversion systems by this drag turbine. The performance of this type of Drag

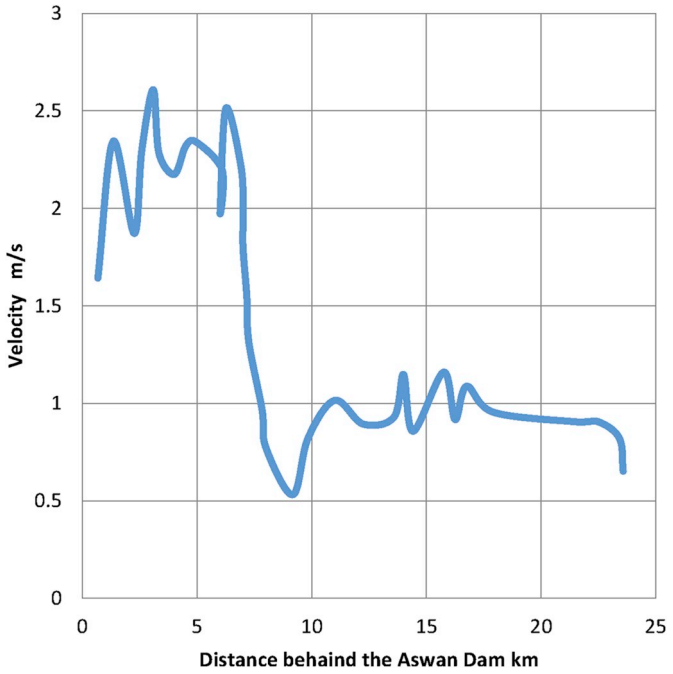

Fig. 5. Water speed vs distance behind Aswan Dam.

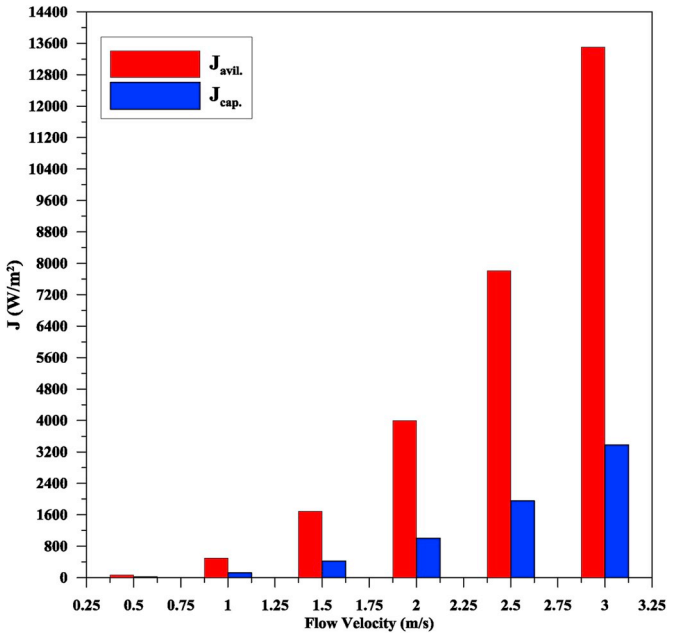

Fig. 6. The power density in river flow.

turbines can be substantially improved by employing multi-objective optimization with its different techniques like GA or MOPSO Algorithms (Ramadan et al., 2018; Mohammadi et al., 2018). Therefore, a lot of authors tried to use multi-objective optimization to improve the performance of this turbine. Actually, multi-objective optimization is used in improving the drag turbine (Ramadan et al., 2018; Mohammadi et al., 2018) and the turbo-machines in general (Polat and Tuncer, 2013; Esmaeilzadeh and Alam, 2019; Mengistu and Ghaly, 2008; Samad and Kim, 2008; HalderMohamed and Samad, 2018; Mohamed et al., 2008a).

This paper aims to investigate the ability to install the Savonius turbine with S shape at the north of Aswan Dam – Aswan city – Egypt. This design is targeting to be an off-grid system as a stand-alone system of electric power production. Authors tested this type of turbine numerically and experimentally at different wind speed, the final result indicated that the power coefficient was 28%. Therefore, it is encouraged us to use it as a hydrokinetic turbine (Mohamed et al., 2008a). The study is performed numerically at different water flow speed according to the selected locations as seen in Fig. (4).

The statistical data of the water speed can be seen in Fig. (5) (Sattar and Raslan, 2014). The data were predicted for 120 days due to the flow rate at these locations. As illustrated and shown in Fig. (6), the available power density ($J_{avil.}$) and captured power density ($J_{cap.}$) of water flow. These parameters are defined as follow:

$$J_{avil.} = \text{Avilable power / rotor area} = 0.5\ \rho\ U_w^3/A \quad (1)$$

$$J_{cap.} = J_{avil.} \times C_p. \quad (2)$$

This type of stand-alone power system could be the core of development in the rural area in Upper Egypt due to the simplicity of the turbine in both manufacturing and installation. Moreover, Table (1) indicates the average annual water level and velocity at 5 different zones with different in river's widths. The flow rate is approximately 250 m^3/s according to the study of Yasser and Radwa (Raslan and Salama, 2015). The system is designed to be flexible in level variation according to the water level. This flexibility is conducted with benefit of installation near to the surface of water and the fixation at the rocks on the small islands in these zones with easily access.

2. Methodology

By using the sliding mesh model (SMM), the two-dimensional unsteady flow is simulated to consider the physics of rotor rotation effects. A double-check on convergence is accomplished; the first convergence criterion is depending on the torque coefficient C_m. As a global convergence criterion, each simulation ends when the difference between the values of the torque coefficient C_m shows a deviation of less than 1% compared with equivalent values of the previous periods. After the fulfillment of the last criterion of convergence, a further convergence check of residuals is set to 10^{-5} with a maximum number of iterations of 200 as 6 iterations per time step of 2π per revolution. Each simulation showed that it may require from 5 up to 15 cycles to reach the quasi-steady state. The initiate of the correct flow solution is carried out in the first cycle, while the flow characteristics, especially the power coefficient C_p and the torque coefficient C_m are calculated by averaging the results during the last two cycles. The current investigation with maximum sub-iterations of 200 to initiate the solution convergence at each time step is used.

A rectangular flow domain with suitable dimensions is adopted while the ratio between the sides flows domain length 45 and width with 25 the rotor diameter as shown in Fig. 7 (Ramadan et al., 2018; El-Baz et al., 2015). An unstructured grid consists of triangular and quadratic elements is adopted for both fixed and rotating flow domains as drawn in Fig. 8. The near-wall region can be divided into three sub layers; the viscous sub-layer, the buffer layer, and the fully turbulent layer. The unstructured grids are substantially increased in the vicinity of wall boundaries, in order to get a normalized wall distance $y+ > 30$. Keeping $y+ > 30$ makes the usage of wall functions is a must. This is achieved by employing 15 boundary layers with a growth rate of 1.2 on all wall surfaces (i.e., turbine shaft and its blades) for open Savonius turbine. Constant inlet velocity is used the simulation and it equals 0.5 m/s as water current and retained constant in all simulations. Symmetry boundary conditions are imposed on both boundary streamlines (i.e., normal derivatives of dependent variables are zero) as appeared in Fig. 7. The interface boundary condition is used on the circumference of the rotating zone to keep the continuity in the flow field.

Table 1
The annual change of the Nile River's current specifications.

Month	W.L	Velocity with 5 m width Zone 1	Energy Flux W/m^2	The velocity with 2.5 m width Zone 2	Energy Flux W/m^2	The velocity with 1.5 m width Zone 3	Energy Flux W/m^2
Jan	69.20	0.72	56.59	1.45	1509.02	2.41	6986.21
Feb	69.99	0.71	182.29	1.43	1458.29	2.38	6751.33
Mar	70.72	0.71	176.74	1.41	1413.92	2.36	6545.94
Apr	71.40	0.70	171.72	1.40	1373.77	2.33	6360.04
May	72.50	0.69	164.02	1.38	1312.14	2.30	6074.70
Jun	72.43	0.69	164.49	1.38	1315.95	2.30	6092.38
Jul	71.97	0.69	167.66	1.39	1341.30	2.32	6209.73
Aug	70.92	0.70	175.18	1.41	1401.45	2.35	6488.18
Sept	70.55	0.71	178.00	1.42	1423.99	2.36	6592.56
Oct	70.20	0.71	180.66	1.42	1445.29	2.37	6691.15
Nov	69.29	0.72	187.84	1.44	1502.70	2.41	6956.94

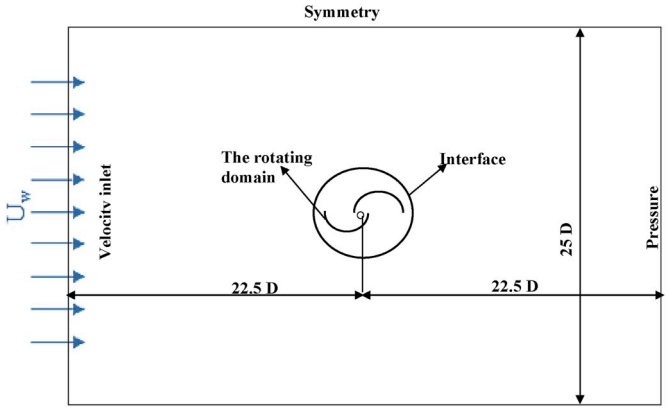

Fig. 7. The Computational domain and boundary conditions.

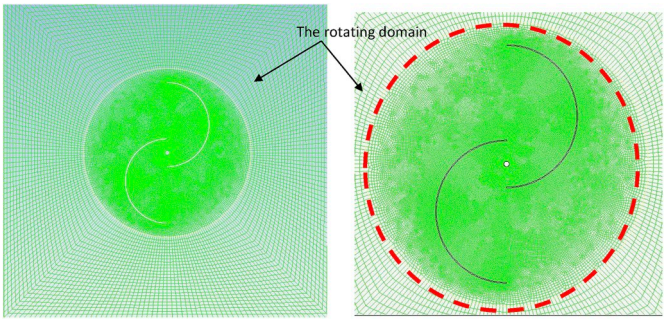

Fig. 8. The Rotating domain.

Table 2
Turbine geometry of conventional and S shape Savonius Turbine and operating parameters.

Parameter	Value	Unit
Turbine S blades Turbine diameter (D)	0.3	m
Conventional Turbine Turbine bucket diameter (d)	0.18	m
Overlap ration (e/D)	0.2	–
Bucket thickness	1	mm
Shaft diameter	6.75	mm

Table 3
The model parameters.

No. of Cells	45000
Domain Size	L/D = 25 and W/D = 25
Turbine Position at Domain	Middle of the domain

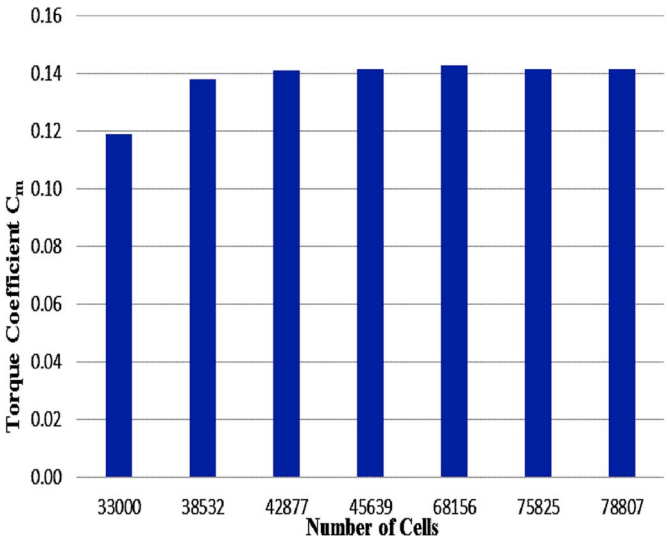

Fig. 9. Grid independence test.

3. Results and discussion

3.1. Validation of the model

A numerical model for Savonius of two blades is conducted with the same dimension as in El-Baz and et al. (El-Baz et al., 2015). The flow field is solved by utilizing the unsteady flow with Sliding Mesh Model (SMM) which is recommended for rotating zones (El-Baz et al., 2015). This model is solved numerically by the commercial finite volume solver ANSYS-Fluent to get the torque coefficient and the power coefficient on the turbine blades. The model is chosen to have the same dimension and the same configuration as in El-Baz and et al. (El-Baz et al., 2015). Therefore, it can be validated easily with their turbine and with the experimental measurements for the same dimension and design for other articles. As presented in Table (2), the geometrical and design parameters are with a schematic description in figs. (7, 8). There are two parameters that have an influence on the performance of any turbine; the torque coefficient C_m and the power coefficient C_p which are written as follows:

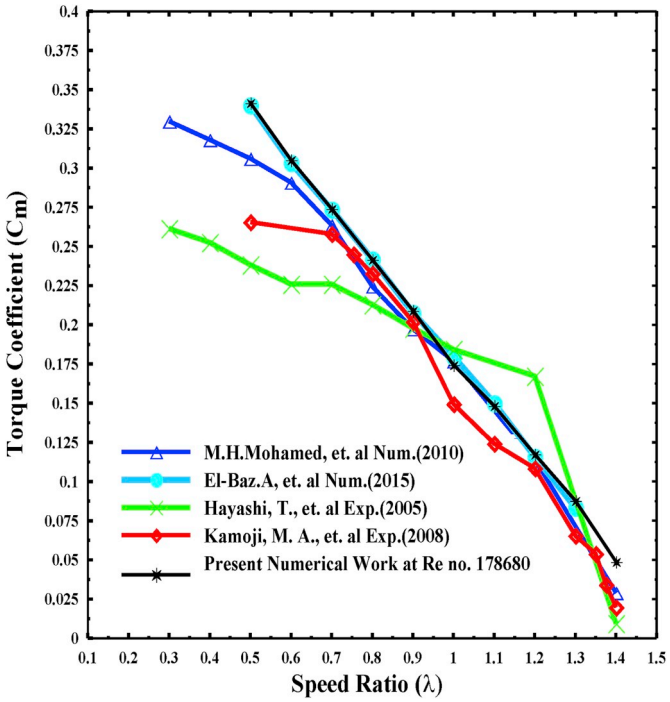

Fig. 10. The torque coefficient validation.

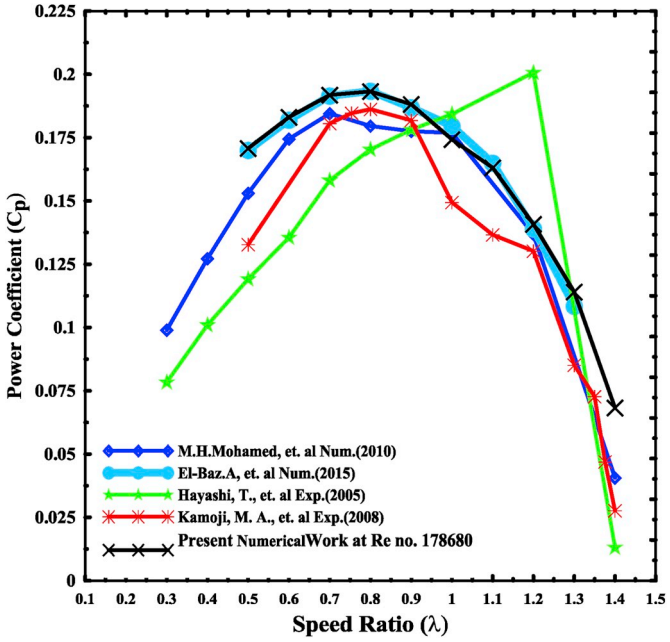

Fig. 11. The power coefficient validation.

$$C_m = \frac{T}{0.5\,\rho U_w^2 A\,R} \tag{3}$$

where T is the average aerodynamic torque acting on the rotor shaft, ρ is the density of the water, U_w is the approaching water speed, A is the frontal area of the turbine, and finally, R is the rotor radius.

$$C_p = \frac{T\omega}{0.5\,\rho U_w^3 A} \tag{4}$$

ω is the angular speed of the rotor.

The tip speed ratio [λ] of the turbine is defined as:

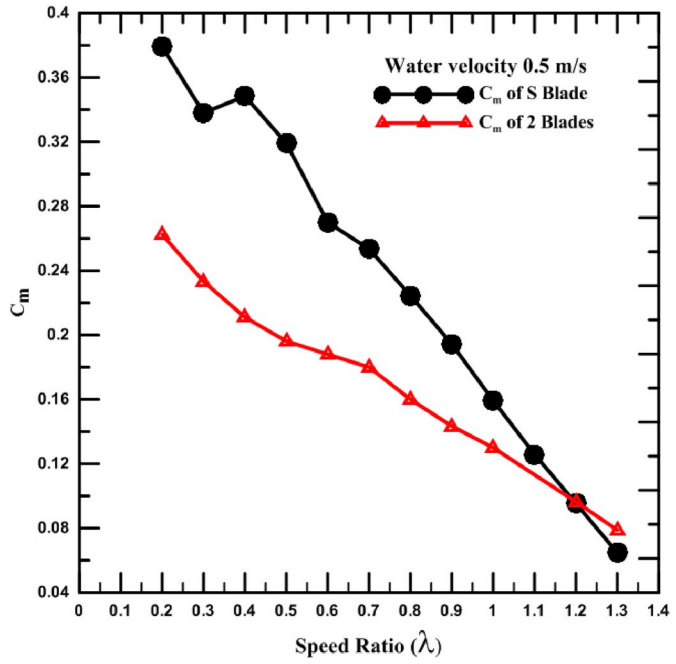

Fig. 12. The torque coefficient of conventional Savonius and S shape numerically.

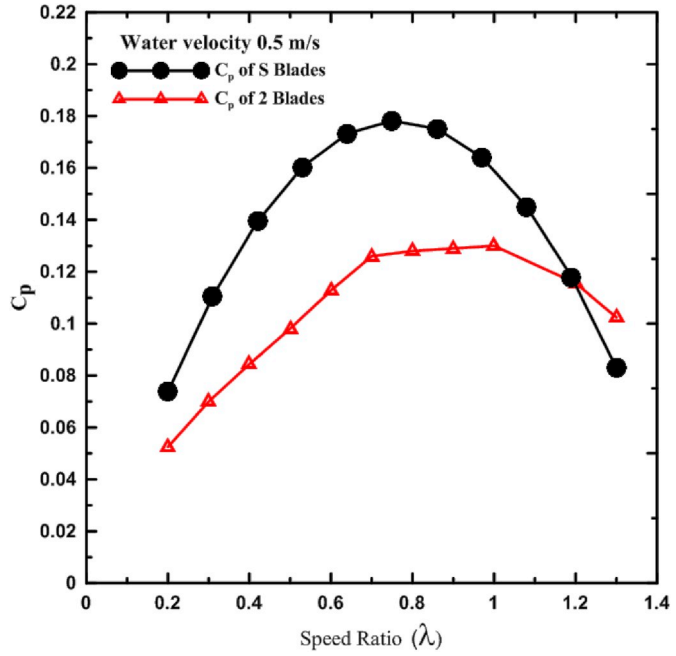

Fig. 13. The power coefficient of conventional Savonius and S shape numerically.

$$\lambda = \frac{R\omega}{U_w} \tag{5}$$

Equation (4) can be rewritten as follows

$$C_p = \lambda\, C_m \tag{6}$$

These terms of power and torque coefficients are calculated at different Reynolds's numbers based on the approaching water speed U_w with kinematic viscosity υ and D is the blade diameter.

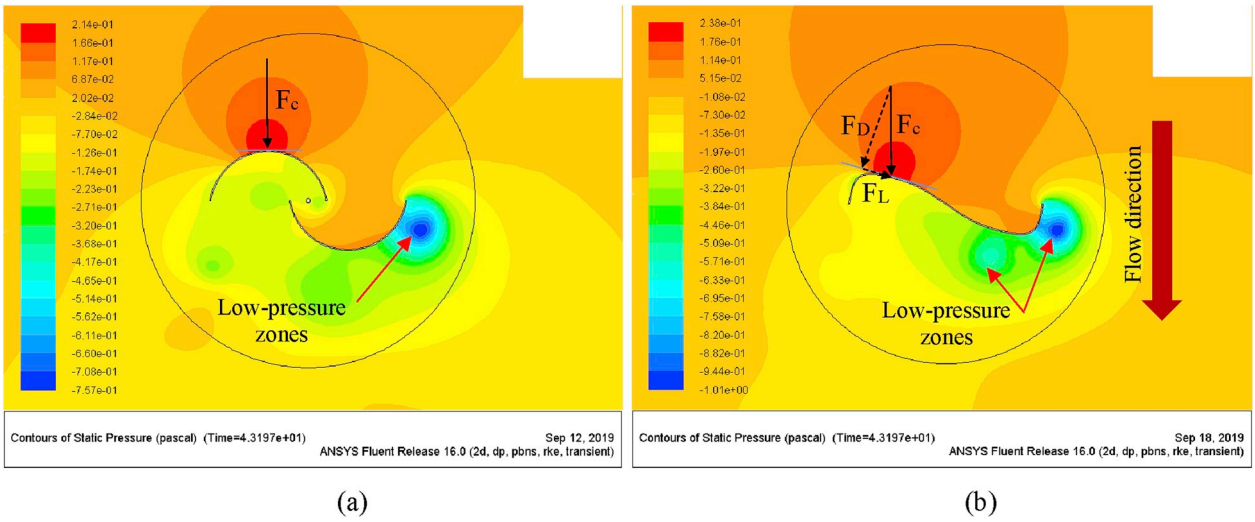

Fig. 14. Static pressure contours of (a) Conventional blade rotor and (b) S shape blade rotor.

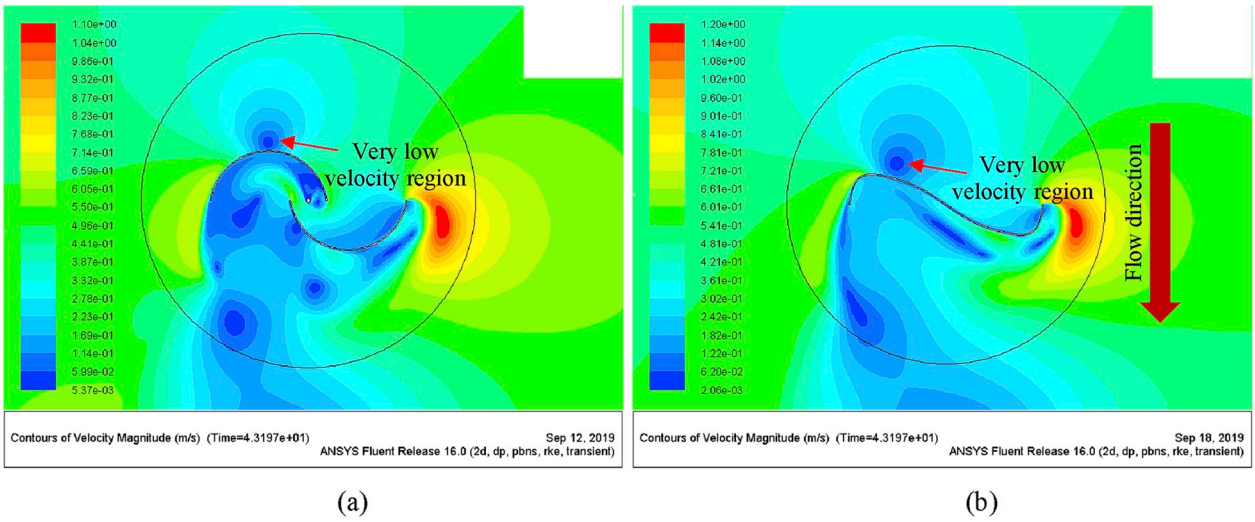

Fig. 15. Velocity contours of (a) Conventional blade rotor and (b) S shape blade rotor.

$$\mathrm{Re} = \frac{D\rho\, U_w}{\upsilon} \tag{7}$$

Table (3) indicates the model specifications for the validation sequences according to El-Baz and et al. (El-Baz et al., 2015). The Realizable $k-\varepsilon$ model with standard wall function is adopted in the current model. K-epsilon (k-ε) turbulence model is the most common model used in Computational Fluid Dynamics (CFD) to simulate mean flow characteristics for turbulent flow conditions. It is a two-equation model that gives a general description of turbulence by means of two transport equations (PDEs). The main references on this model are described by Jones and Launder (1972) and Launder and Sharma (1974). The original impetus for the K-epsilon model was to improve the mixing-length model, as well as to find an alternative to algebraically prescribing turbulent length scales in moderate to high complexity flows https://en.wikipedia.org/wiki/K-epsilon_turbulence_model (Bardina et al., 1997).

The k-ε model has been tailored specifically for planar shear layers https://en.wikipedia.org/wiki/K-epsilon_turbulence_model - cite_note-5and recirculating flows. This model is the most widely used and validated turbulence model with applications ranging from industrial to environmental flows, which explains its popularity. It is usually useful for free-shear layer flows with relatively small pressure gradients as well as in confined flows where the Reynolds shear stresses are most important. It can also be stated as the simplest turbulence model for which only initial and/or boundary conditions needs to be supplied. K-ε model also performs satisfactorily in a variety of important cases such as unconfined flows https://en.wikipedia.org/wiki/K-epsilon_turbulence_model (Bradshaw, 1987), curved boundary layers, rotating flows and flows in non-circular ducts, https://en.wikipedia.org/wiki/K-epsilon_turbulence_model (Larsson et al., 2011). A set of equations which can be applied to a large number of turbulent applications are (Versteeg and Malalasekera, 2007):

For turbulent kinetic energy k

$$\frac{\partial(\rho k)}{\partial t} + \frac{\partial(\rho k u_i)}{\partial x_i} = \frac{\partial}{\partial x_i}\left[\frac{u_t}{\sigma_k}\frac{\partial k}{\partial x_i}\right] + 2\mu_t E_{ij}E_{ij} - \rho\varepsilon \tag{8}$$

For dissipation

$$\frac{\partial(\rho\varepsilon)}{\partial t} + \frac{\partial(\rho\varepsilon u_i)}{\partial x_i} = \frac{\partial}{\partial x_j}\left[\frac{u_t}{\sigma_\varepsilon}\frac{\partial \varepsilon}{\partial x_j}\right] + C_{1\varepsilon}\frac{\varepsilon}{k}2\mu_t E_{ij}E_{ij} - C_{2\varepsilon}\rho\frac{\varepsilon^2}{k} \tag{9}$$

$$\mu_t = C_\mu \rho \frac{k^2}{\varepsilon} \tag{10}$$

where constants are: $C_\mu = 0.09$, $\sigma_k = 1$, $\sigma_\varepsilon = 1.3$, $C_{1\varepsilon} = 1.44$ $C_{2\varepsilon} = 1.92$.

The domain is split into two zones, the stationary and rotating zones.

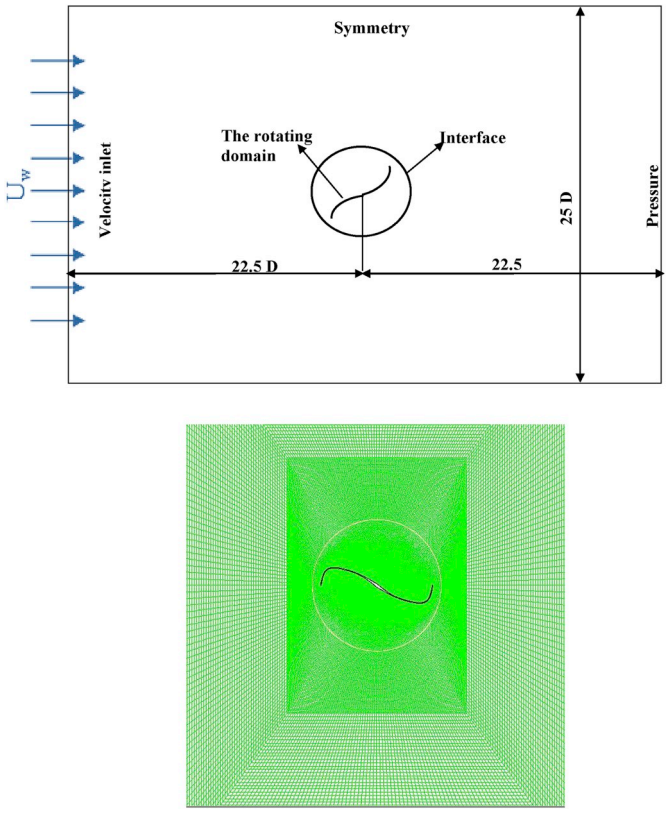

Fig. 16. The computational Domain and Boundary Condition.

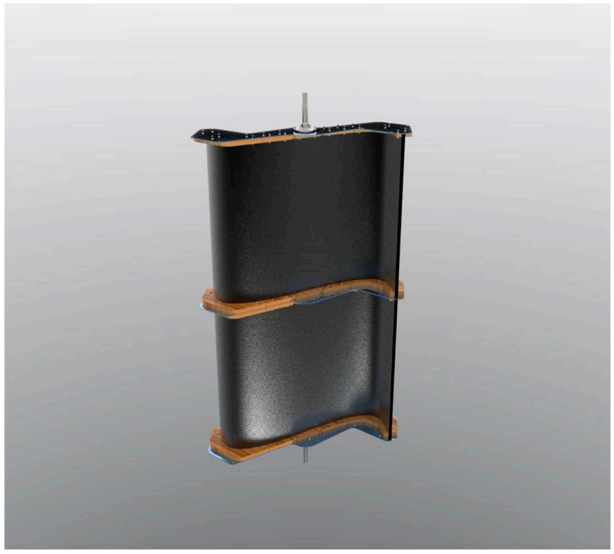

Fig. 17. The S shape for the Savonius turbine.

The stationary zone domain embraces the water velocity inlet, pressure outlet, and the symmetry sides. The suited mesh technique used is obtained in fig. (4) near to the turbine blade (high intensive mesh zone).

The enhanced wall function method is applied to ensure the precise resolution of the boundaries layer prediction (El-Baz et al., 2015).

The wall function approach needs the dimensionless distance of the first grid point from the wall (y+ (it is a non-dimensional **distance** (based on local cell fluid velocity) from the wall to the first mesh node)) to be greater than 30; this is used to the present work.

Fig. (9) illustrates the grid independence test at tip speed ratio equal

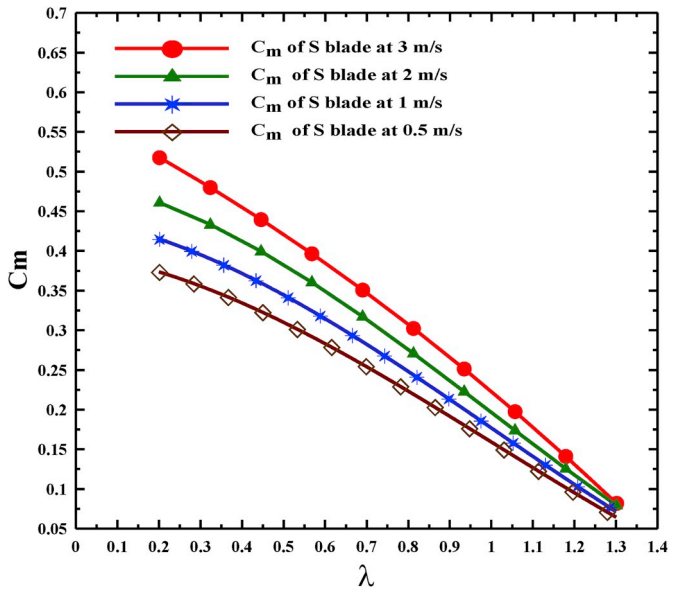

Fig. 18. The Torque Coefficient versus Tip speed ratio.

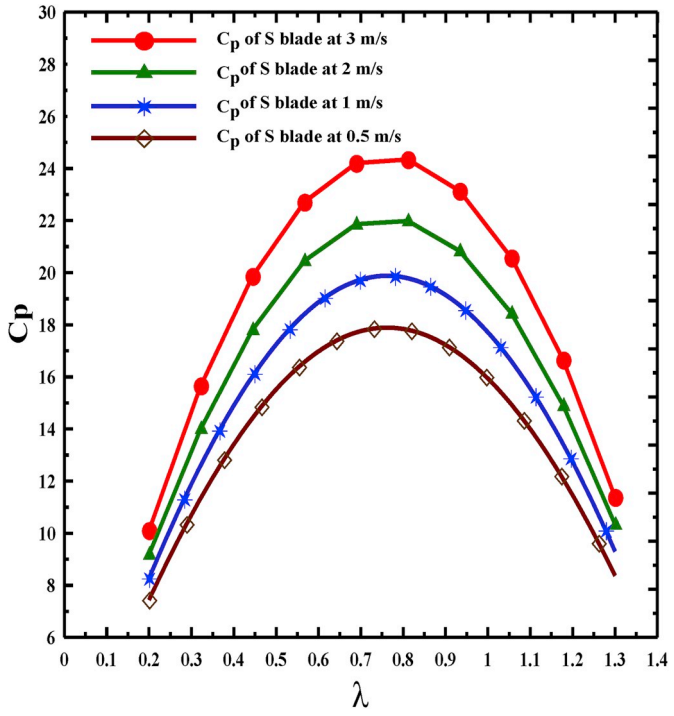

Fig. 19. The Power Coefficient versus Tip speed ratio.

to 1 with the torque coefficient. The grid independency is checked for different cell numbers, which ranged from 33000 to 79000. The torque coefficient becomes stable and constant after 45639 cells. Moreover, the time step size is considered as in El-Baz and et al. (El-Baz et al., 2015), to validate the model with the same specification.

As in Figs. 10 and 11, the present model results show a convincing agreement with the experiments for both power and torque coefficients. The performance and the design of the Savonius rotor rely on some parameters like the number of blades, the number of stages and the geometry of the blades. Until now, there is still no exact theoretical procedure to estimate the performance of the Savonius drag rotor.

The most preferable way of optimizing the different parameters is to

perform a number of experiments on different types of rotors in a low-speed open test section wind tunnel. Fig. (10) is showing the torque coefficient C_m comparison between the present numerical investigations for 2 blades Savonius turbine with Kamoji et al. (2008) (Re = 155000) and Hyashi et al. (Hayashi et al., 2005) as (Re = 210000).

As a result of the convergence appeared in fig. (10) and fig. (11) between the numerical works with other authors, it encourages us to use the numerical model and create a numerical model with S shape to be the hydrokinetic turbine. The S shape is used in this type of turbine because of the high performance, compared to the conventional Savonius turbine (Ramadan, 2016; Mohamed et al., 2008b). The numerical work is showing preliminary outcomes compared to the conventional Savonius with two rotors (Figs. 12 and 13). The efficiency of the S shape turbine reaches 18% approximately instead of 12% for conventional Savonius. This enhancement in power is due to the increase in the lifting force on the blade with highly negative pressure.

In Fig. 14a, the hydrokinetic momentum creates a high-pressure zone located on the reversed blade of the conventional rotor. This high-pressure zone affects adversely the reversed rotor blade by a concentrated force (F_c) perpendicular to such blade. This force generates an adverse torque that reduces the rotor performance. On the other hand, the same force F_c has been created on the reversed blade of the S shape rotor. However, according to the designed geometry of the blade, the F_c is analyzed into two force components Drag force component (F_D) and Lift force component (F_L). The F_D is perpendicular to the tangent of the reversed S shape blade and F_L is tangential to the reversed S shape blade as shown in Fig. 14 (b). The F_D component generates an adverse torque less than that generated on the conventional rotor. Consequently, the net torque generated on the blade increased obviously as shown in Fig. 12. The novelty of the S-shape advanced blade is that only a component of this concentrated force acts in a direction opposing rotor rotation. This lift force F_L component enhances the power captured by the rotor. Also, the S shape advanced blade has a two low pressure zones rather than the conventional one as shown in Fig. 14 (a) and (b). The novelty of the S-shape reversed blade is that only a component of this concentrated force acts in a direction opposing rotor rotation. This gives preference to the S shape rotor to capture more power. The velocity contours for conventional and S shape rotor blades are shown in Fig. 15 (a) and (b), respectively. A very low velocity region exists, accompanied by the high-pressure zones where the flow becomes semi-stagnant and acts as a brake.

3.2. Numerical analysis of the S shape

The numerical model is rebuilt with the S shape turbine with the same dimension of the validated conventional Savonius. Fig. (16) illustrates and shows the meshed model and the computational domain with the different boundary conditions of the inlet and outlet of the domain for the S shape. The numerical study is performed with a water speed of 0.5, 1, 2, and 3 m/s to investigate the power and torque coefficients and how these speeds influence the performance of the turbine. Fig. (17) is showing the suggested S blade turbine design to get the maximum power as possible from the incident water flow.

3.3. Numerical results of the S shape

Fig. (18) illustrates the output torque coefficient of the S blade turbine at different tip speed ratios. The indicated results in this fig. are the usual for this kind of the Savonius turbine, thus the torque coefficient decreases with an increase in the tip speed ratio. Fig. 18 introduces the power coefficient with the different tip speed ratios at various water flow speed. The optimum power coefficient is found at a tip speed ratio of 0.8, which is 24.6%. At tip speed ratio 0.8, the flow streamlines are stickier on the blade suction side surface and the separation of the flow is less at this value. Hence, it is considered as the optimum operating performance at turbine maximum speed. At this tip speed ratio, the blade captured more lifts and drags from the flow with higher value of lift to drag ratio, which leads directly to an increase in the power coefficient. Moreover, the pressure variation at this tip speed ratio is more than the other tip speed ratios. As shown in Fig. (19), the increase in the water flow speed increases the power coefficient due to the power stored in the high flow velocity.

4. Conclusion

The current paper investigates the possibility to use the S shape blade for the hydrokinetic turbine to be a stand-alone power electric station. This model is solved numerically by the commercial finite volume solver ANSYS-Fluent to get the torque coefficient and the power coefficient on the turbine blades. The proposed location of installation of this kind of turbine is at Upper Egypt – Aswan city-behind the Aswan Dam. The streamflow velocity at this location is in the range from 1 to 3 m/s. The most significant findings are summarized as follows:

- The numerical analysis indicates that the S shape blade has the maximum power coefficient of 24.6% for a tip speed ratio 0.8 and streamflow velocity 3 m/s.
- The more the streamflow velocity, the more the maximum power coefficient at a tip speed ratio of 0.8.
- The results indicate that the maximum power coefficient of the new design (S-shape) and the conventional design are 18% and 12.8% at the tip speed ratio 0.8 and streamflow velocity 0.5 m/s, respectively.
- The new design (S-shape) enhance the turbine performance by 40% compared with the conventional design, especially at low stream flow velocity.
- These premium results encourage the authors to work more to enhance the efficiency by getting the optimum turbine and efficiency for these locations.

Due to these promising results, the main hope of the present work is the spreading of this turbine along the river Nile coast in Upper Egypt for the required development there.

Acknowledgment

Interesting discussions, with Eng. Alaa El Feky CEO of Blue Power Company is appreciated by the authors.

Nomenclature

C_m	The torque coefficient
C_p	The power coefficient
T	The average aerodynamic torque (N.m)
ρ	The density of the water (kg/m3)
Re	Reynolds number
U_w	The approaching water speed (m/s)
A	The frontal area of the turbine (m^2)
R	The rotor radius (m)

ω	The angular speed of the rotor (rad/s)
λ	The tip speed ratio of the turbine
υ	kinematic viscosity (m^2/s)
D	The blade diameter (m)
J_{avil}	The available power density (W/m^2)
J_{cap}	The captured power density (W/m^2)
u_i	Velocity Component (m/s)
E_{ij}	Rate of Deformation
μ_t	Eddy Velocity
k	Turbulence Kinetic Energy
ε	Rate of Dissipation
w. L Fc	Water Line Concentrated Force (N)
F_D	Drag Force (N)
F_L	Lift Force (N)

References

Antheaume, S., Maitre, Thierry, Achard, Jean-Luc, 2008. Hydraulic Darrieus turbines efficiency for free fluid flow condition versus power farms condition. Renew. Energy 33, 2186–2198.

Bardina, J.E., Huang, P.G., Coakley, T.J., 1997. Turbulence Modeling Validation, Testing, and Development. NASA Technical Memorandum, p. 110446.

Bradshaw, P., 1987. Turbulent secondary flows. Annu. Rev. Fluid Mech. 19, 53–74.

Chris Schleicher, W., Riglin, Jacop D., Kraybill, Zachary A., Oztekin, Alparslan, Klein Jr., Robert C., 2013. "Design and Simulation of a Micro Hydrokinetic Turbine," in 1st Marine Energy Technology Symposium.

El-Baz, A.R., Youssef, K., Nabil, A., Hamed, A.M., 2015. Optimization of two and three rotor Savonius wind turbine. In: ASME Turbo Expo 2015: Turbine Technical Conference and Exposition. American Society of Mechanical Engineers.

Esmaeilzadeh, Soheil, Alam, Mohammad-Reza, 15 February 2019. Shape optimization of wave energy converters for broadband directional incident waves. Ocean Eng. 174, 186–200.

Halder, Paresh, Mohamed, M.H., Samad, Abdus, 2018. Wave energy conversion: design and shape optimization. Ocean. Eng. 150, 337–351.

Hantoro, R., Prananda, J., Mahmashani, A.W., Septyaningru, E., Imanuddin, F., 2018. "Performance investigation of an innovative vertical Axis hydrokinetic turbine – straight blade cascaded (VAHTSBC) for low current speed". J. Phys. Conf. Ser. 1022, 012022.

Hayashi, Tsutomu, Li, Yan, Hara, Yutaka, 2005. Wind tunnel tests on a different phase three-stage Savonius rotor. JSME Int. J. Ser. B Fluids Therm. Eng. 48 (1), 9–16.

Jones, W.P., Launder, B.E., 1972. The prediction of laminarization with a two-equation model of turbulence. Int. J. Heat Mass Transf. 15, 301–314.

Kamoji, M.A., Kedare, S.B., Prabhu, S.V., 2008. Experimental investigations on single stage, two stage, and three stage conventional Savonius rotor. Int. J. Energy Res. 32 (10), 877–895.

Kumar, Anuj, Saini, R.P., August 1, 2017. Performance analysis of a Savonius hydrokinetic turbine having twisted blades. Renew. Energy 108 (Suppl. C), 502–22.

Larsson, I.A.S., Lindmark, E.M., Lundström, T.S., Nathan, J.G., 2011. Secondary flow in semi circular ducts. Trans. ASME J. Fluids Eng. 133, 101206–101214.

ABS alaskan Inc. report, january 2010 siting considerations for kinetic (In-Stream) hydro turbines. http://www.abşak.com/tech/EnCurrentSiting.pdf.

Launder, B.E., Sharma, B.I., 1974. Application of the energy dissipation model of turbulence to the calculation of flow near a spinning disc. Lett. Heat Mass Transf. 1 (2), 131–138.

Mengistu, Temesgen, Ghaly, Wahid, September 2008. Aerodynamic optimization of turbomachinery blades using evolutionary methods and ANN-based surrogate models. Optim. Eng. 9 (3), 239–255.

Mohamed, M.H., 2011. Design Optimization of Savonius and Wells Turbine. Ph.D. Thesis. University of Magdeburg "Otto von Guericke", Germany.

Mohamed, M.H., Janiga, G., Thévenin, D., 2008. "Performance Optimization of a Modified Wells Turbine Using Non-symmetric Airfoil Blades", ASME Turbo Expo 2008: Power for Land, Sea, and Air, Berlin.

Mohamed, M.H., Janiga, G., Thévenin, D., 2008. "Performance Optimization of a Modified Wells Turbine Using Non-symmetric Airfoil Blades", ASME Turbo Expo 2008: Power for Land, Sea, and Air, Berlin.

Mohammadi, M., Lakestani, M., Mohamed, M.H., January 15, 2018. Intelligent parameter optimization of Savonius rotor using artificial neural network and genetic algorithm. Energy 143 (Suppl. C), 56–68.

Polat, Ozge, Tuncer, Ismail H., 2013. Aerodynamic shape optimization of wind turbine blades using a parallel genetic algorithm. Procedia Eng. 61, 28–31.

Ramadan, A., 2016. Innovative design investigation of an augmented drag vertical Axis wind turbine under unsteady characteristics. In: Proc. Of the 4th International Conference and Exhibition on Mechanical & Aerospace Engineering, pp. 1–19.

Ramadan, A., Yousef, K., Said, M., Mohamed, M.H., 2018. Shape optimization and experimental validation of a drag vertical axis wind turbine. J. Energy 151, 839–853.

Raslan, Yasser, Salama, Radwa, 2015. Development of Nile River islands between old aswan Dam and new esna barrages. Water Sci. J. 29, 77–92.

Samad, A., Kim, K.-Y., 2008. Shape optimization of an axial compressor blade by multi-objective genetic algorithm. Proc Inst. Mech. Eng. A J. Power Energy.

Sarma, N.K., Biswas, A., Misra, R.D., 2014. Experimental and computational evaluation of Savonius hydrokinetic turbine for low velocity condition with comparison to Savonius wind turbine at the same input power". J. Energy Convers. Manag. 83, 88–89.

Sattar, Ahmed M.A., Raslan, Yasser M., January 1, 2014. Predicting morphological changes DS new naga-hammadi barrage for extreme nile flood flows: a Monte Carlo analysis. J. Adv. Res. 5 (1), 97–107.

Sharma, Kaushal Kumar, Gupta, Rajat, Biswas, Agnimitra, March 20, 2014. Performance measurement of a two-stage two-bladed Savonius rotor. Int. J. Renew. Energy Resour. 4 (1), 115–21.

Tutar, Mustafa, Veci, Inaki, 2015. Experimental wave flume study of savonius-type multiple rotor arrays. J. Renew. Sustain. Energy 7 (6), 063125. November 1.

Verdant Power, June, 2006. Technology Evaluation of Existing and Emerging Technologies- Water Current Turbines for River Applications.

Versteeg, Henk Kaarle, Malalasekera, Weeratunge, 2007. An Introduction to Computational Fluid Dynamics: the Finite Volume Method. Pearson Education.

Yaakob, Omar, Arif Ismail, M., Ahmed, Yasser M., 2013. Parametric study for Savonius vertical Axis marine current turbine using CFD simulation. Latest Trends Renew. Energy Environ. Inf. Conf.

Zaidi, Mahrukh, Uddin, Naseem, Adeel, Asma, 2013. Numerical simulations of hydrokinetic turbine for power generation. Proc. Int. Energy Sustain.